JACS
JOURNAL OF THE AMERICAN CHEMICAL SOCIETY
Article
pubs.acs.org/JACS

Carbon–Hydrogen Activation of Cycloalkanes by Cyclopentadienylcarbonylrhodium—A Lifetime Enigma

Amanda L. Pitts,[†] Alisdair Wriglesworth,[‡] Xue-Zhong Sun,[‡] James A. Calladine,[‡] Snežana D. Zarić,[§,⊥] Michael W. George,*[,‡] and Michael B. Hall*[,†]

[†]Department of Chemistry, Texas A&M University, College Station, Texas 77843-3255, United States
[‡]School of Chemistry, University of Nottingham, University Park NG7 2RD, U.K.
[§]Science Program, Texas A&M University at Qatar, Doha, Qatar
[⊥]Department of Chemistry, University of Belgrade, 11000 Belgrade, Serbia

Supporting Information

ABSTRACT: Carbon–hydrogen bond activation reactions of four cycloalkanes (C_5H_{10}, C_6H_{12}, C_7H_{14}, and C_8H_{16}) by the Cp′Rh(CO) fragments (Cp′ = η^5-C_5H_5 (Cp) or η^5-C_5Me_5 (Cp*)) were modeled theoretically by combining density functional and coupled cluster theories, and their reaction rates were measured by fast time-resolved infrared spectroscopy. The reaction has two steps, starting with the formation of a σ-complex intermediate, followed by oxidative addition of the C–H bond by the rhodium. A range of σ-complex stabilities among the electronically unique C–H bonds in a cycloalkane were calculated and are related to the individual strengths of the C–H bond's interactions with the Rh fragment and the steric repulsion that is incurred upon forming the specific σ-complex. The unexpectedly large increase in the lifetimes of the σ-complexes from cyclohexane to cycloheptane was predicted to be due to the large range of stabilities of the different σ-complexes found for cycloheptane. The reaction lifetimes were simulated with two mechanisms, with and without migrations among the different σ-complexes, to determine if ring migrations prior to C–H activation were influencing the rate. Both mechanisms predicted similar lifetimes for cyclopentane, cyclohexane, and, to a lesser extent, cycloheptane, suggesting ring migrations do not have a large impact on the rate of C–H activation for these cycloalkanes. For cyclooctane, the inclusion of ring migrations in the reaction mechanism led to a more accurate prediction of the lifetime, indicating that ring migrations did have an effect on the rate of C–H activation for this alkane, and that migration among the σ-complexes is faster than the C–H activation for this larger cycloalkane.

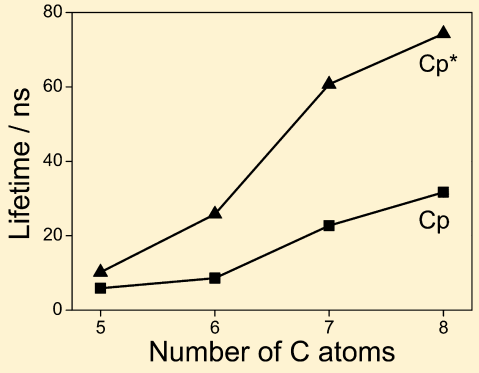

INTRODUCTION

Two separate groups first reported alkane C–H bond activation by a metal center, where an unsaturated metal oxidatively added an alkane C–H bond to form an alkyl hydride.[1,2] There is extensive evidence in the literature that the key intermediate in this process is a σ-complex, where an alkane binds to an unsaturated 16-electron metal center.[3−6] Such σ-complexes have been characterized by crystallography[7] and low-temperature NMR,[8−13] which support previous experiments using infrared spectroscopy.[14−18] In particular, time-resolved infrared (TRIR) spectroscopy used in conjunction with metal carbonyl complexes (for their narrow and intense ν(CO) infrared bands) has proven useful in monitoring ultrafast reactions, such as C–H activation at room temperature.[19,20] Organometallic complexes such as Cp′Rh(CO)$_2$ (Cp′ = η^5-C_5H_5 (Cp), η^5-C_5Me_5 (Cp*)) have been instrumental in developing an understanding of C–H activation reactions.[21−25]

Previous low-temperature experiments using small concentrations of alkane in liquefied rare gas media reported C–H activation of the alkane by Cp*Rh(CO)$_2$ following photolysis.[21,22] After initial formation of a rare gas complex, an equilibrium was established with the alkane σ-complex. Increasing the size of the alkane shifted the equilibrium in favor of the alkane complex, which also affected the kinetics of the subsequent C–H activation reaction.

Although monitoring the vibrational stretching frequencies of metal carbonyls has given insight into the overall reaction mechanism, computational methods are needed to resolve the finer picture.[26−34] Eisenstein and co-workers published calculated free energy values for propane reacting with a TpRh(CNR) fragment.[35] They found a lower activation barrier for the primary C–H bonds than for the secondary C–H bonds of propane, and a low barrier for the 1,2-migration from the methylene to the methyl group. This led to the conclusion that the methylene activation would occur less frequently than a migration from the methylene to the methyl group.[35] It had been assumed that the migration in longer alkanes proceeded by a series of 1,2-migrations; however, the recent study by

Received: February 11, 2014
Published: May 13, 2014

   dx.doi.org/10.1021/ja5014773 | J. Am. Chem. Soc. 2014, 136, 8614−8625

Table 1. Calculated Free Energies (kcal mol^{-1}) for the Cyclohexane Reaction with CpRh(CO)

	σ-complex[a]		activation barrier[b]		product[b]	
	axial	equatorial	axial	equatorial	axial	equatorial
BP86	−0.24	−0.32	5.12	4.39	−2.44	−4.13
BMK	−0.02	0.37	10.97	9.95	−0.09	−2.79
B3LYP	2.52	2.43	10.73	9.79	3.19	1.22
B97D	−4.44	−3.73	4.97	4.97	−3.92	−5.02
M06-L	−2.73	−2.15	9.64	9.68	1.83	1.14
ωB97XD	−5.15	−4.55	9.29	8.89	2.39	0.81
PBE	−1.82	−1.76	4.78	4.03	−2.70	−4.26
TPSS	−0.38	−0.38	6.10	5.36	−2.78	−4.30
CCSD(T)//BMK[c]	−6.78	−6.34	6.64	6.40	−8.04	−9.46

[a]Relative to the free reactants. [b]Relative to the σ-complex. [c]Calculated by adding BMK's free energy correction to the CCSD(T) electronic energies.

George et al.[23] showed that 1,3-migrations have lower energy barriers. As such, 1,3-migrations were predicted to occur before C−H activation even more readily than 1,2-migrations for these longer alkanes. Also, for propane and longer alkanes, the methyl groups' activation barriers were calculated to be constant, so the lifetime trends were a reflection of the varying migration rate down the chain and not the energetics of the C−H activation step.[23] Since the terminal CH_3 groups on linear alkanes were the dominant groups being activated, attention was turned toward cycloalkanes, which do not possess any primary C−H bonds to be activated. Initial studies using cyclopentane and cyclohexane, with a combined experimental and theoretical approach, showed a stronger binding enthalpy for alkanes with CpRh(CO) than with Cp*Rh(CO). It was concluded that the difference in activation rate was mainly due to steric crowding caused by the bulkier Cp* ligand; however, a migration mechanism was not investigated.[24]

In the study presented here, cyclopentane and cyclohexane reacting with the two Rh fragments (CpRh(CO) and Cp*Rh(CO)) are revisited along with cycloheptane and cyclooctane, yielding eight reactions in total. Room-temperature lifetimes have been reported and activation parameters obtained for all the reactions by ns-TRIR and variable-temperature experiments. Additionally, for each reaction a migration mechanism and a second reaction pathway referred to as the static mechanism, where no migration transfers are included, were simulated in a kinetic model and theoretical lifetimes determined. These predicted lifetimes for both mechanisms were then compared with the experimental lifetimes to determine which mechanism best describes the C−H activation of the cycloalkanes.

EXPERIMENTAL SECTION

Materials and Methods. Cp*Rh(CO)$_2$ was purchased from Strem Chemicals, Inc. and used as received. CpRh(CO)$_2$ was synthesized via a reported procedure.[36] Cyclopentane (Sigma-Aldrich, ≥99%), cyclohexane (Sigma-Aldrich, ≥99.9%), cycloheptane (Alfa Aesar, 99%), and cyclooctane (Alfa Aesar, 99%) were dried by refluxing over CaH_2 under an argon atmosphere prior to use. CO (BOC, CP grade) was used as received.

The concentrations of the samples were typically in the range 10^{-3}−10^{-4} M, and experiments were performed under an atmosphere of CO (ca. 2 atm). For all of the TRIR measurements, a variable-temperature transmission IR cell (Harrick Scientific Products, Inc.) was used, with CaF_2 windows (25 × 2 mm) at a path length of 0.5 mm. Teflon tubing and a peristaltic pump were used to circulate the sample. A water jacket surrounding the cell was connected to a recirculating water bath to control the temperature of the cell, which was monitored using a 1/16-in. thermocouple permanently sealed into the solution. This allowed for constant measurement of the cell temperature to within 0.1 °C. A temperature range of 5−60 °C was used for the experiments.

The ultrafast TRIR apparatus is discussed elsewhere,[37] so only a brief summary is provided here. A combination of a Ti:sapphire oscillator and a regenerative amplifier system was used to produce 800 nm laser pulses. This output was used to pump an optical parametric amplifier (OPA) followed by a difference frequency generator (DFG) unit to generate a tunable mid-IR pulse. A Ge beam splitter was used to separate the mid-IR pulse, with a small portion going to a single-element mercury−cadmium−telluride (MCT) detector to be used as a reference (i.e., to allow normalization to take into account shot-to-shot fluctuation). The rest of the beam was used as the probe and traveled through the sample. A 250 mm IR monochromator with 150 L/mm gratings (giving ca. 4 cm^{-1} resolution) dispersed the transmitted IR beam onto an MCT array detector with 128 elements. The signals were amplified with a 144-channel amplifier and digitized by a 16-bit analog-to-digital converter.

For the ns-TRIR experiments, the output of a Q-switched Nd:YVO laser (1064 nm) was passed through a frequency-quadrupling crystal (i.e., 266 nm output) and used as the pump. This was synchronized to the Spitfire Pro amplifier (Spectra-Physics), and the delay was controlled by a pulse generator (DG535, Stanford Research Systems), allowing delays from 0.5 ns to 100 μs to be used.

Computational Details. All theoretical calculations were performed with the Gaussian 09 suite of programs.[38] A survey of functionals was conducted for the cyclohexane reaction with BMK,[39] B3LYP,[40,41] ωB97XD,[42] TPSS,[43] BP86,[44,45] PBE,[46,47] B97D,[48] and M06-L,[49] using the 6-311++G**[50,51] basis set for the C, H, and O atoms and the Stuttgart quasi-relativistic basis set and effective core potential[52] for Rh. The cyclohexane reaction was chosen because cyclohexane was the smallest cycloalkane that had more than one type of σ-complex and activation barrier; for axial and equatorial C−H bonds, see Table 1. BP86 and B3LYP calculated the equatorial σ-complex to be more stable than the axial; PBE, ωB97XD, B97D, M06-L, and BMK calculated the axial σ-complex to be more stable than the equatorial;[8c] and TPSS calculated the two σ-complexes to be equal in energy. Since it was unknown which σ-complex was experimentally more stable for this reaction and the functionals did not consistently calculate the axial/equatorial energy difference, single-point CCSD(T)[53] calculations with the same basis set as that used for the DFT calculations (above) were performed for the cyclohexane reaction, with starting geometries from the converged BMK and TPSS geometry optimization calculations. The CCSD(T)//BMK and CCSD(T)//TPSS single-point calculations predicted the axial σ-complex to be more stable than the equatorial species, and of the five functionals that predicted this trend, BMK paralleled the relative energy of the CCSD(T) single-point calculations the best. The ωB97XD functional, which was shown in previous work to calculate accurate trends for these reactions[24] and would account for the dispersion in the Cp*Rh(CO) reactions, was not used because of geometry optimization issues with the larger cycloalkanes. Since the BMK results are scaled using CCSD(T), which includes dispersion, additional dispersion corrections on the DFT would make little

dx.doi.org/10.1021/ja5014773 | J. Am. Chem. Soc. 2014, 136, 8614−8625

difference. The BMK functional was thus chosen to calculate the reaction mechanisms for this work. Although the BMK functional calculated accurate free energy trends, the free energy barriers were not accurate when compared to the CCSD(T) calculations. Therefore, the BMK free energy barriers were scaled by the multiplicative scaling factor from the electronic energy ratio E_e(BMK)/E_e(CCSD(T)//BMK) for the respective barrier (see Supporting Information). The activation barriers for the CpRh(CO) reactions were scaled by a factor of 0.68, while those for the Cp*Rh(CO) reactions were scaled by a factor of 0.73, and the migration barriers for all eight reactions were scaled by a factor of 1.24. The initial barrier between the separated species and the σ-complex, referred to here as the attachment barrier, was taken to be 4.00 kcal mol^{-1} (k = 7.22 × 10^9 s^{-1}) because the calculations showed no electronic energy barrier for this attachment. Thus, the barrier (rate constant) was largely dependent on the diffusion of the Rh fragment in the reaction medium and the corresponding loss of entropy in the attachment of the alkane. Although counterpoise corrections are important for such attachment energies, they were not included in the BMK or CCSD(T) calculations because the C−H activation barriers and migration barriers were the main focus of the study. Since the geometry does not undergo a large change when moving from the σ-complex to either of these transition states (TSs) on the potential energy surface, counterpoise corrections would not have a significant effect on the energies.[23] Since these neutral molecules are in nonpolar solvents, all reported values are scaled gas-phase free energies, unless otherwise noted, and no corrections for concentration were made (see Supporting Information).[35] Each species was optimized in the gas phase with tight convergence criteria and on an ultrafine grid as specified in Gaussian 09. Analytical frequency calculations were performed on all optimized structures to ensure that either a minimum or a first-order saddle point was achieved. 3D molecular structures displayed in this article were drawn with the JIMP2 molecular visualization and manipulation program.[54]

Chemical Kinetics Simulator. The kinetics simulator[55] used a stochastic algorithm to propagate a reaction and produce an output of the reaction species' concentration versus time. Reaction rates were calculated from transition state theory and fed into the simulator, from which the lifetimes were computed with the proportional relationship between the product's half-life and lifetime. The separated species were used as the initial reactants with an attachment barrier of 4.00 kcal mol^{-1}, and the reverse dissociation reaction was not included in the simulation. The final products from the C−H activation reaction of each unique σ-complex were added together to give an overall final product concentration for each reaction's simulation, which was then used to calculate the lifetimes. For the migrations between σ-complexes, both the forward and reverse reactions between the complexes were included.

EXPERIMENTAL RESULTS AND DISCUSSION

ns-TRIR spectra of CpRh(CO)$_2$ were obtained following irradiation (266 nm) in a cyclooctane solution under a CO atmosphere, Figure 1. Within the time resolution of the experiment (0.5 ns), the parent bands at 1982 and 2046 cm^{-1} bleached and a transient band at 1959 cm^{-1} was formed. This transient band decayed within ca. 50 ns to yield another band at 2014 cm^{-1} on the same time scale. The photochemistry of CpRh(CO)$_2$ in alkane solvent has been studied in detail, and these bands can be assigned to the σ-complex CpRh(CO)(alkane) and the alkyl hydride CpRh(CO)(alkyl)(H), respectively.[21−25] When the transition metal complex was changed to Cp*Rh(CO)$_2$, the profiles of the ns-TRIR spectra in cyclooctane were very similar: the only significant change was a down-shift in the frequencies associated with the σ-complex and alkyl hydride, to 1938 and 1995 cm^{-1}, respectively.

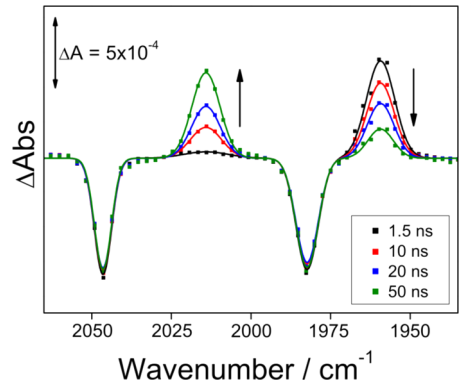

Figure 1. ns-TRIR spectra of CpRh(CO)$_2$ in cyclooctane under a CO atmosphere, at selected time intervals following photolysis (266 nm).

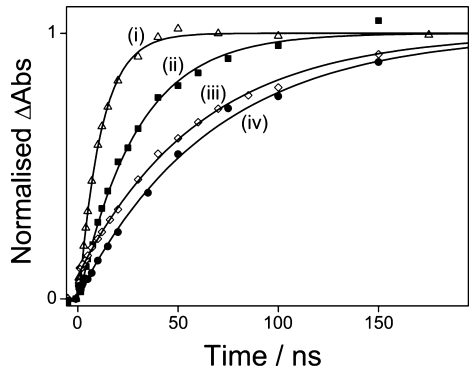

Figure 2. Normalized TRIR single-point kinetic traces showing the formation of the alkyl hydride Cp*Rh(CO)(alkyl)(H) obtained following photolysis (266 nm) under a CO atmosphere in (i) cyclopentane, (ii) cyclohexane, (iii) cycloheptane, and (iv) cyclooctane.

Single-point kinetic traces following the formation of the alkyl hydride complexes of the Cp*Rh(CO) fragment in the various cyclic solvents were also obtained, Figure 2. All the traces fitted to a monoexponential growth, which is consistent with the unimolecular C−H activation step. As the size of the cyclic alkane increases, there is a decrease in the rate of C−H activation. For the linear alkanes this trend has been well documented and discussed.[23] Interplay between activation at primary C−H bonds and multiple migration pathways along the chain to the terminal CH_3 group appears to cause the observed decrease in rate with increasing chain length. However, for the cyclic alkanes there are only secondary C−H bonds to be activated and migration pathways are less facile; therefore, different factors may be controlling the rate.

The lifetimes of C−H activation for cycloheptane/cyclooctane were relatively similar to each other, as were those of cyclopentane/cyclohexane, Figure 3. For Cp*Rh(CO), a lifetime of 10.2 ± 0.8 ns was obtained in cyclopentane, and for cyclohexane it increased slightly to 25.8 ± 2.0 ns. However, for cycloheptane there was a significant change in lifetime to 60.7 ± 2.4 ns, and there was another small rise to 74.3 ± 4.0 ns upon increasing the size of the alkane to cyclooctane. A similar but less pronounced step-like trend was also observed for CpRh(CO), showing how the nature of the alkane is a key factor in determining the rate. The results indicate a clear difference between the two systems, with much slower rates of C−H activation obtained for Cp*Rh(CO) compared with CpRh(CO). This is in contrast to the linear alkanes, where

dx.doi.org/10.1021/ja5014773 | J. Am. Chem. Soc. 2014, 136, 8614−8625

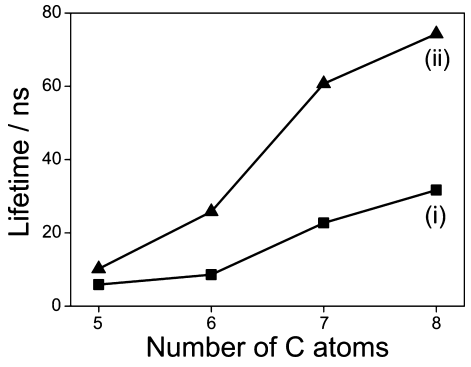

Figure 3. Plot of lifetimes for the C−H activation of cycloalkanes as a function of the number of C atoms in the cyclic alkane: (i) $CpRh(CO)_2$ and (ii) $Cp^*Rh(CO)_2$.

both complexes have similar rates.[23] Therefore, the slower rate for Cp*Rh(CO) with cyclic alkanes is proposed to be due to the increased steric bulk of the cyclic alkane interacting with the more sterically hindered Cp* compared to Cp.

To probe the factors controlling these experimental lifetimes, activation parameters were obtained from variable-temperature ns-TRIR experiments (5−60 °C), Table 2. The observed activation energies (E_a) showed poor correlation to the measured lifetimes, especially for Cp*Rh(CO), revealing the complicated nature of the C−H activation process. Eyring analysis offers some insight, but the trends in $\Delta H^{\ddagger}$ and $\Delta S^{\ddagger}$ are not dramatic, and the differences are marginally significant, particularly given the difficulties in obtaining precise values.[56,57] First of all, negative entropies of activation ($\Delta S^{\ddagger}$) are consistent with a rate-determining unimolecular oxidative addition step, while relatively small enthalpies of activation ($\Delta H^{\ddagger}$) indicate an early TS with limited C−H bond-breaking character.[22] The results obtained here for the Cp*Rh(CO) fragment can be compared to those obtained from previous studies in low-temperature liquefied krypton doped with alkane,[21,22] and the magnitudes of the $\Delta H^{\ddagger}$ and $\Delta S^{\ddagger}$ reported here were similar. However, a more detailed comparison is not possible due to the larger errors in the previous studies and the observed pre-equilibrium with a krypton complex influencing the overall C−H activation parameters. Despite the fact that some information can be gained from these variable-temperature TRIR experiments, calculations are needed in order to gain a much more detailed insight into the mechanism of C−H activation for these alkanes, especially as to what role migrations have within the reaction.

QUANTUM CHEMICAL CALCULATIONS

Reaction Scheme. There are two general steps in the C−H activation of cycloalkanes with the Cp′Rh(CO) fragments, Scheme 1. The first step forms a C−H σ-complex from the separated cycloalkane and Cp′Rh(CO) fragment, and the second step is oxidative addition breaking the C−H bond and forming new Rh−C and Rh−H bonds. However, as observed with linear alkane C−H activation, since migrations can occur between σ-complexes before activation occurs, this basic two-step mechanism is transformed into a multistep one. For migrations to be important, their energy barriers should be lower than those for the activations, and for migrations to affect the lifetime, different C−H bonds in the cycloalkanes need to have different activation energies. The free energy of the ring migration barriers relative to those for activation and the plausibility of ring migrations altering the lifetime, are herein addressed for all eight reactions. The barriers described below are all scaled free energy barriers for the activations and migrations.

Scheme 1. Potential Energy Diagram for the Reaction of Cp′Rh(CO) with a Cycloalkane

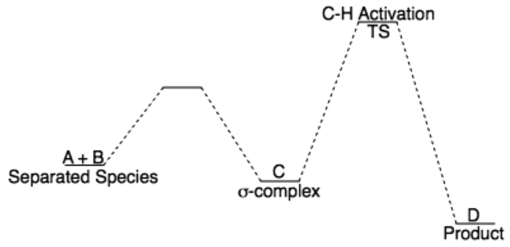

Reactants. The six reactants were optimized individually to determine their lowest energy conformations and to compare their electronic structures. Cp* is a stronger electron donor than Cp because of its methyl groups, Figure 4, as reflected in stronger and shorter Rh−C bonds, and by a longer C−O bond for the Cp*Rh(CO) fragment, Table 3. Therefore, it might be predicted that this fragment would form a more stable σ-complex because of more back-donation from the rhodium into the C−H σ-antibonding orbital. However, it is more sterically crowded due to the bulkier Cp*, which offsets this stabilizing effect. The four cycloalkanes were individually optimized in their most stable conformation, Figure 5. For cyclopentane this was the envelope that has C_s symmetry with four CH_2 groups in a plane and the fifth puckered out of the plane, which results in

Table 2. Arrhenius and Eyring Activation Parameters for CpRh(CO) and Cp*Rh(CO) with Cycloalkanes; Lifetimes at 298 K Are Included for Clarity

	E_a (kcal mol^{-1})	$\Delta H^{\ddagger}$ (kcal mol^{-1})	$\Delta S^{\ddagger}$ (cal K^{-1} mol^{-1})	τ^{298} (ns)[a]
		CpRh(CO)		
cyclopentane	3.24(±0.19)	2.65(±0.19)	−12.0(±0.5)	5.9(±0.2)
cyclohexane	3.47(±0.15)	2.86(±0.15)	−12.0(±0.5)	8.6(±0.3)
cycloheptane	4.80(±0.09)	4.20(±0.09)	−9.46(±0.3)	22.7(±0.7)
cyclooctane	4.43(±0.22)	3.82(±0.21)	−11.4(±0.7)	31.7(±0.9)
		Cp*Rh(CO)		
cyclopentane	4.14(±0.42)	3.55(±0.42)	−10.1(±1.2)	10.2(±0.8)
cyclohexane	4.80(±0.41)	4.80(±0.41)	−9.77(±1.36)	25.8(±2.0)
cycloheptane	4.58(±0.19)	4.58(±0.19)	−12.2(±0.6)	60.7(±2.4)
cyclooctane	4.34(±0.29)	4.34(±0.29)	−13.4(±0.93)	74.3(±4.0)

[a]Errors were calculated using ±σ from linear regression.

dx.doi.org/10.1021/ja5014773 | J. Am. Chem. Soc. 2014, 136, 8614−8625

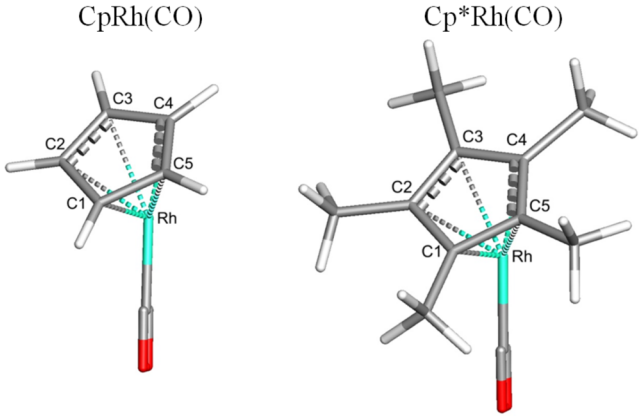

Figure 4. Optimized geometries for the CpRh(CO) and Cp*Rh(CO) fragments.

Table 3. Bond Distances between Rh and Ligands on CpRh(CO) and Cp*Rh(CO)

bond	CpRh(CO)	Cp*Rh(CO)
Rh−C1	2.113	2.099
Rh−C2	2.271	2.274
Rh−C3	2.300	2.291
Rh−C4	2.298	2.292
Rh−C5	2.277	2.274
average	2.252	2.246
Rh−C	1.866	1.864
C−O	1.144	1.148

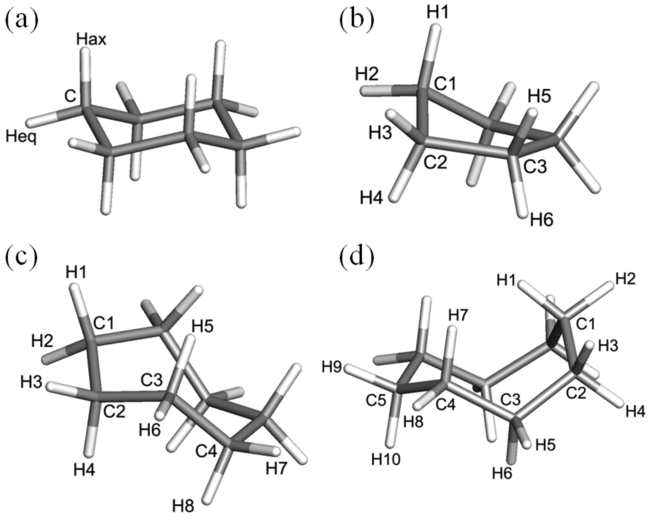

Figure 5. Lowest energy conformations for each cycloalkane with the different C−H groups denoted.

six different C−H bonds. The chair conformation is the most stable geometry for cyclohexane, which has 2 unique C−H bonds, axial and equatorial. Cycloheptane maintains a C_2 axis in the twisted chair conformation, which has 7 different C−H bonds, and cyclooctane has C_s symmetry in the boat-chair geometry with 10 unique C−H bonds. Table 4 lists the various calculated C−H bond lengths for the free cycloalkanes; the stability of the σ-complexes was influenced by the cycloalkane's C−H bond strength with lower energy σ-complexes resulting when the Rh fragment binds to weaker (longer) C−H bonds.

Table 4. C−H Bond Distances in the Separated Cycloalkanes

cyclopentane		cyclohexane	
C1−H1	1.0974	C−Hax	1.0989
C1−H2	1.0939	C−Heq	1.0958
C2−H3	1.0937		
C2−H4	1.0964		
C3−H5	1.0943		
C3−H6	1.0933		
cycloheptane		**cyclooctane**	
C1−H1, C1−H2	1.0969	C1−H1	1.0959
C2−H4	1.0973	C1−H2	1.0970
C2−H3	1.0959	C2−H3	1.0979
C3−H5	1.0985	C2−H4	1.9800
C3−H6	1.0961	C3−H5	1.0959
C4−H8	1.0987	C3−H6	1.0944
C4−H9	1.0970	C4−H7	1.0975
		C4−H8	1.0960
		C5−H9	1.0974
		C5−H10	1.0991

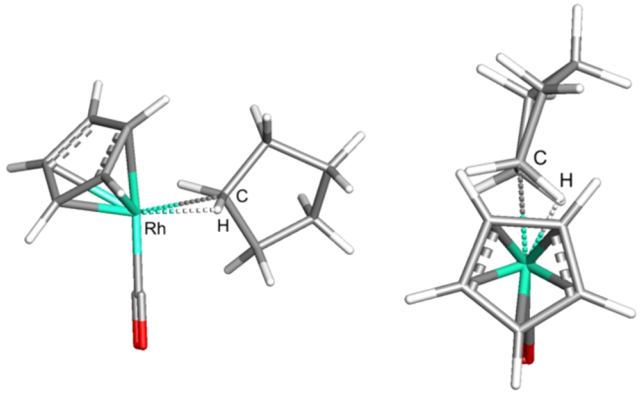

Figure 6. Side and top views of the only stable cyclopentane σ-complex found.

CpRh(CO) Reactions. A σ-complex structure was calculated for each C−H bond for all four cycloalkanes to confirm that unique C−H bonds form distinct intermediates (see Supporting Information). In every case, the σ-complex has its bound C−H bond oriented perpendicular to the Rh−C−O vector. For cyclohexane, cycloheptane, and cyclooctane, distinct intermediates were formed, but the six different C−H bonds in cyclopentane all converged to the same σ-complex. When any of the six different C−H bonds binds to the Rh center, the cyclopentane rearranges by puckering the CH_2 group opposite from the bound C−H bond, Figure 6. Unlike the rest of the calculated cycloalkanes, only cyclopentane activates this electronically unique C−H bond, as its rearrangement energy is so low. The free energy of activation for the σ-complex was predicted to be 5.94 kcal mol^{-1}, which is the only barrier influencing the lifetime of this reaction, because ring migrations are redundant in this case.

For cyclohexane, the reaction can proceed through two distinct C−H bonds, axial and equatorial. The equatorial bond was the stronger C−H bond in cyclohexane and had a calculated bond distance of 1.096 Å, while the axial bond was slightly weaker and longer at 1.099 Å. Due to the difference in bond strengths, the σ-complexes that form from these two bonds are not energetically equivalent. The axial species was

dx.doi.org/10.1021/ja5014773 | J. Am. Chem. Soc. 2014, 136, 8614−8625

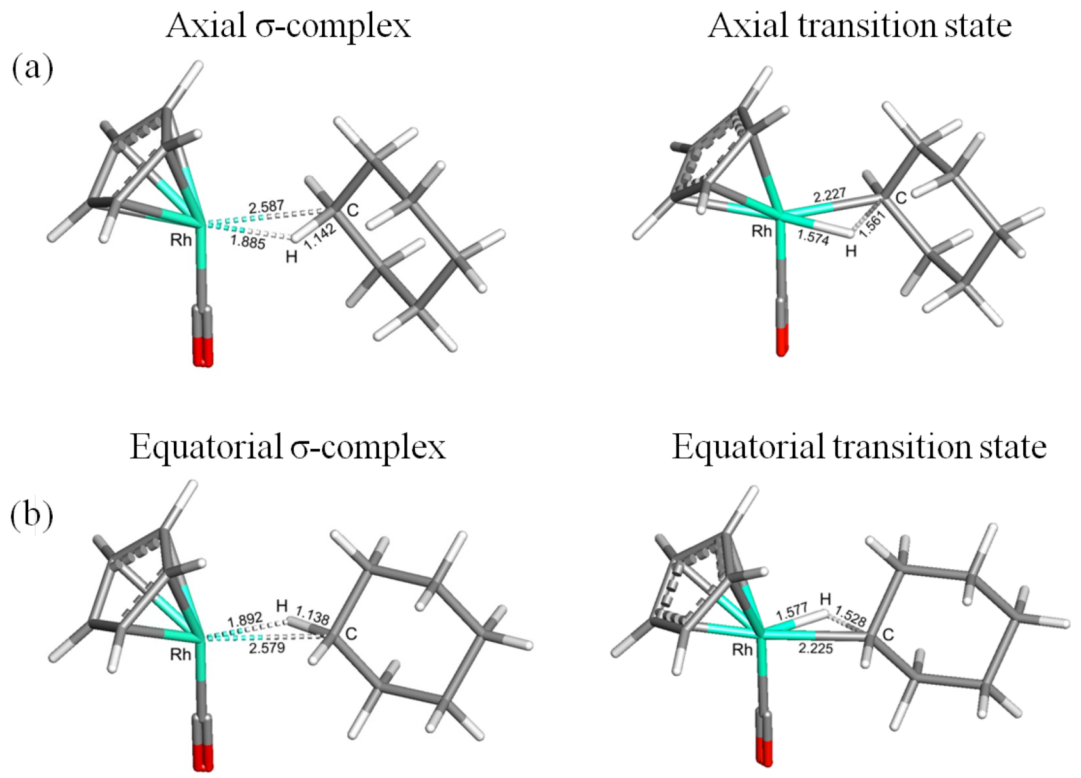

Figure 7. Optimized geometries for the cyclohexane reaction with CpRh(CO): (a) axial and (b) equatorial C−H activation.

determined to be 0.07 kcal mol^{-1} more stable on the free energy surface than its equatorial counterpart, and this energy difference was reflected by the longer C−H bond for the axial σ-complex intermediate, Figure 7. This result is consistent with previous experimental work by Ball and co-workers, which determined that CpRe(CO)$_2$(cyclohexane) preferentially binds cyclohexane through the axial C−H bond.[8c] Furthermore, the longer C−H bond in the axial complex relates to more electron density transfer between the two fragments, as the longer C−H bond is effectively a better donor (less stable occupied MO) and better acceptor (more stable unoccupied MO). Variations in energy were also observed for the TSs that follow the σ-complexes; however, the equatorial TS was found to be lower in energy than the axial one, 6.52 and 6.97 kcal mol^{-1} for the BMK-scaled values, respectively. The equatorial path has an earlier TS, denoted by the shorter C−H bond distance of 1.528 Å compared to the axial one of 1.561 Å (Figure 7), which is consistent with the lower energy activation barrier. Decreased steric repulsion in the TS for the equatorial activation is proposed as the cause of the earlier TS and lower free energy of activation.

Since the two σ-complexes have different activation barriers, this reaction could be influenced by a ring migration. The two types of ring migrations that were calculated in cyclohexane are the 1,1- and the 1,2-migrations, Figure 8. The former is the transfer between the two C−H bonds on the same carbon, which is a conversion between the axial and equatorial σ-complexes and has a barrier of less than 1 kcal mol^{-1} in either direction. The latter is a transfer between adjacent CH$_2$ groups on the ring, which occurs only between equivalent C−H bonds, as axial to equatorial (or vice versa) has too much steric repulsion. The barriers for these migrations, 7.97 and 12.00 kcal mol^{-1} for equatorial and axial 1,2-migrations, respectively, were predicted to be higher in energy than either of the activation barriers, but because they occur only between equivalent C−H bonds, these migrations are effectively redundant. Therefore, the rapid 1,1-migrations will be the only type of migration affecting the cyclohexane reaction. The barriers for boat-chair rearrangement for cyclohexane and similar rearrangements for the larger cycloalkanes are all greater than the barriers for C−H activation reactions and do not play a role in these reactions.

Increasing the ring by one CH$_2$ group increases the number of possible σ-complexes from two to seven, and, as with cyclohexane, the σ-complexes of cycloheptane have different stabilities. Although the energies of the cyclohexane σ-complexes can be rationalized by the strengths of the interacting C−H bonds, the cycloheptane σ-complex stabilities are not as straightforward. Two factors determine the stability of each intermediate: the strength of the specific C−H bond and the sterics associated with the Rh fragment binding to it. Sterics play a larger role in the stability of cycloheptane σ-complexes because the twisted chair conformation that was maintained in each intermediate caused the ring to have various proximities to the Rh fragment. Intermediates where the ring was turned into the Rh fragment were less stable than those with the ring pointed away, Figure 9. Coupling sterics with the varying C−H bond strengths creates the range of σ-complex energies shown in Table 5, and the possibility for the cycloheptane lifetime to be altered by the addition of ring migrations. The free energies of activation for the seven σ-complexes ranged from 6.88 to 7.46 kcal mol^{-1}. Ring migrations could decrease the lifetime of the overall reaction by populating the σ-complex with the 6.88 kcal mol^{-1} activation barrier and depopulating the intermediates with higher activation barriers.

There are four different types of migrations that can occur for the cycloheptane σ-complex: 1,1-, 1,2-, 1,3-, and 1,4-migrations, as shown in Figure 8. Again, 1,1-migrations had low energy

dx.doi.org/10.1021/ja5014773 | J. Am. Chem. Soc. 2014, 136, 8614−8625

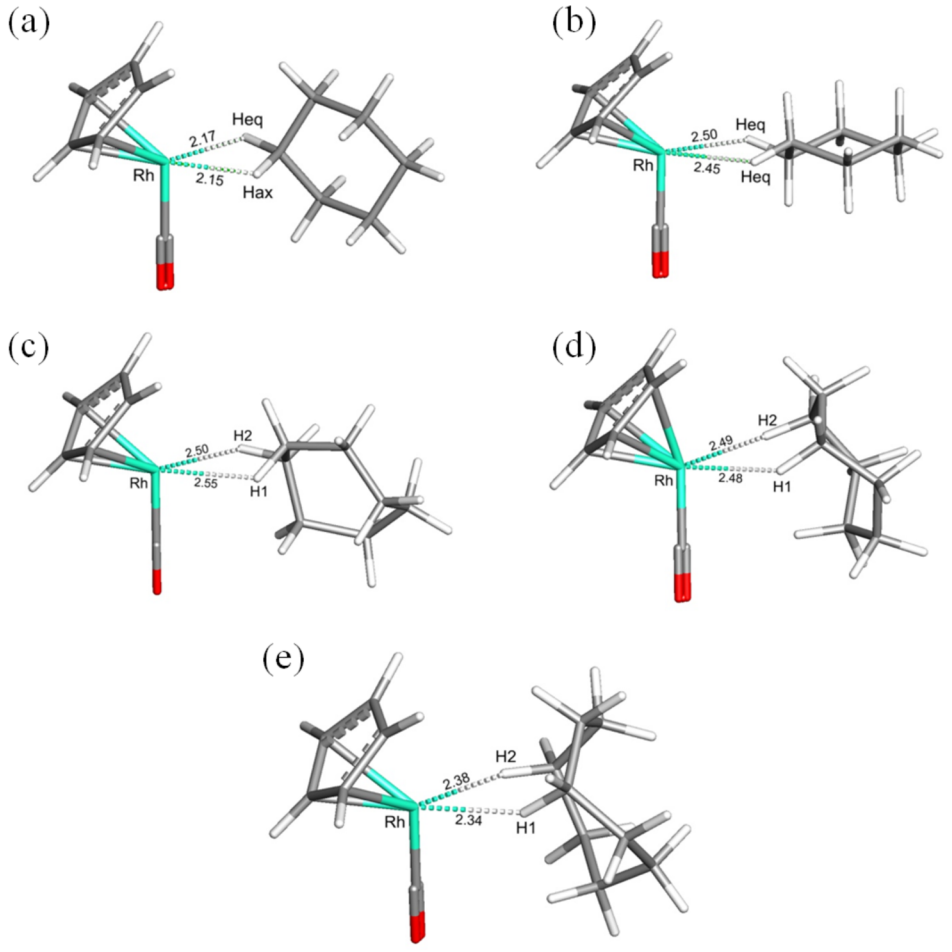

Figure 8. Examples of calculated migration transition states for the CpRh(CO) reactions: (a,b) cyclohexane, (c,d) cycloheptane, and (e) cyclooctane. (a) The 1,1-migration, the transfer between the two hydrogen atoms on one carbon. (b) The interior−interior 1,2-migration, the transfer between two adjacent C−H bonds with a H−C−C−H dihedral angle less than 60°. (c) The interior−exterior 1,2-migration, the transfer between two adjacent C−H bonds with a H−C−C−H dihedral angle larger than 60°. (d) The 1,3-migration, the transfer across the face of the cycloalkane. (e) The 1,4-migration, which is similar to the 1,3-migration but is a transfer to a carbon four CH_2 groups away.

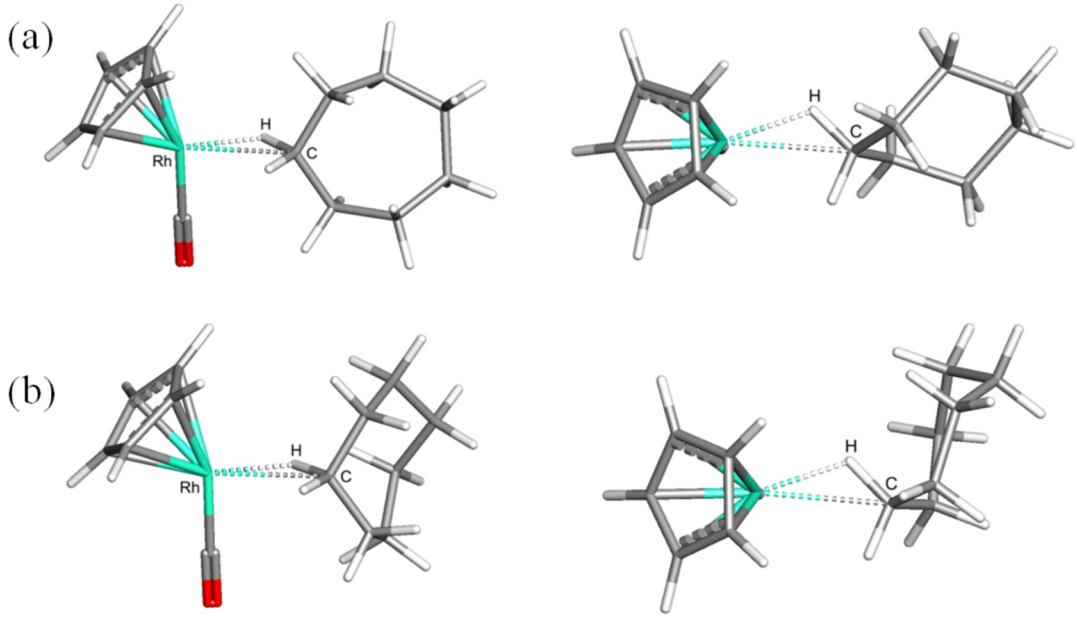

Figure 9. (a) C(1)−H(1) and (b) C(3)−H(5), the most stable and the least stable cycloheptane σ-complexes, respectively. Top and side views are shown for the two σ-complexes.

dx.doi.org/10.1021/ja5014773 | J. Am. Chem. Soc. 2014, 136, 8614−8625

barriers of ca. 1 kcal mol^{-1}, and the two intermediates connected by a 1,1-migration were therefore assumed to be in equilibrium. Unlike cyclohexane, there were two types of 1,2-migrations for cycloheptane, and they depended on the orientation of the adjacent CH_2 units. If the H−C−C−H dihedral angle formed by the two C−H bonds involved in the migration is less than 60°, a 1,2-migration occurs between two interior σ-complexes, but if the dihedral angle is larger than 60°, a 1,2-migration occurs between an interior and an exterior σ-complex, Scheme 2 and Figure 8. The interior−interior 1,2-migration barriers range from 7.54 to 7.72 kcal mol^{-1}, while the interior−exterior 1,2-migration barriers range from 4.52 to 10.19 kcal mol^{-1}. The larger range for the interior−exterior 1,2-migrations is due to the lower stability of the exterior σ-complexes, which are ca. 3−4 kcal mol^{-1} less stable than the interior σ-complexes. Thus, migrating to an exterior σ-complex is more difficult, with an energy range from 8.06 to 10.19 kcal mol^{-1}, while the reverse movement to an interior σ-complex is easier, with an energy range from 4.52 to 7.34 kcal mol^{-1}. The 1,3- and 1,4-migrations were similar in appearance because they required the Rh fragment to transfer across the face of the ring, and their energy barriers range between 7.06 and 7.93 kcal mol^{-1}. Unlike cyclohexane, cycloheptane has numerous non-redundant migration barriers that are smaller than many of its activation barriers. Thus, with a larger range of values for both barriers, these two pathways could compete and affect the overall rate.

Increasing in size again to cyclooctane causes the number of stable σ-complexes to rise from 7 to 10. Again, all 10 σ-complexes had stabilities derived from the combination of sterics and the C−H bond strengths; however, the stabilities of these 10 σ-complexes vary more than those of the previous cycloalkanes. For example, the relative energy difference between the most stable and least stable σ-complexes for cycloheptane was 0.29 kcal mol^{-1}, while for cyclooctane it was 0.90 kcal mol^{-1}. This difference is due, in large part, to the increased steric repulsion caused by the rigidity of the unbound portion of the cyclooctane ring, Figure 10. This larger variation in σ-complex stabilities could lead to migrations having a more significant effect on the rate of C−H activation. For cyclooctane, there are the same four types of possible migrations to consider, and the migration barriers were similar in energy to the cycloheptane energies. The 1,1-migrations had low barriers ranging from 0.02 to 1.89 kcal mol^{-1}; therefore, the two σ-complexes connected by a 1,1-migration were assumed to be in equilibrium again. Of the 1,2-migrations, only interior−exterior ones could be determined with cyclooctane because of the H−C−C−H dihedral angles that were present in the boat-chair conformation. The exterior σ-complexes were again ca. 3−4 kcal mol^{-1} less stable than the interior complexes; the free energy range for these migrations was 4.30−6.10 kcal mol^{-1} to an interior σ-complex and 7.81−10.32 kcal mol^{-1} to an exterior σ-complex. An energy range from 7.18 to 8.64 kcal mol^{-1} was obtained for the 1,3- and 1,4-migrations. The free energies of activation ranged from 6.58 to 9.96 kcal mol^{-1}, which was the largest range of the four cycloalkanes. Interestingly, cyclooctane's smallest activation barrier is less than the corresponding barrier for either cycloheptane or cyclohexane, while increases in steric repulsion pushed other activation barriers to even higher energies. With the larger range of C−H activation energies, migrations between different CH_2 groups could have an even larger impact on the rate of cyclooctane.

Table 5. Relative Free Energies (kcal mol^{-1}) for the Seven σ-Complexes in the Cycloheptane Reaction, with Zero Relative Energy Being the Most Stable Species

activated C−H bond[a]	CpRh(CO)	Cp*Rh(CO)
C1−H1, C1−H2	0.00	0.00
C2−H3	0.14	0.87
C2−H4	0.20	0.86
C3−H5	0.43	1.47
C3−H6	0.35	0.79
C4−H7	0.31	0.72
C4−H8	0.24	1.39

[a]See Figure 4 for numbering scheme.

Scheme 2. σ-Complex Geometries and 1,2-Migrations: Interior (Rh Attached between the Two H's on a CH_2 Group) and Exterior (Rh Attached to One C−H Bond on the Ring Side)

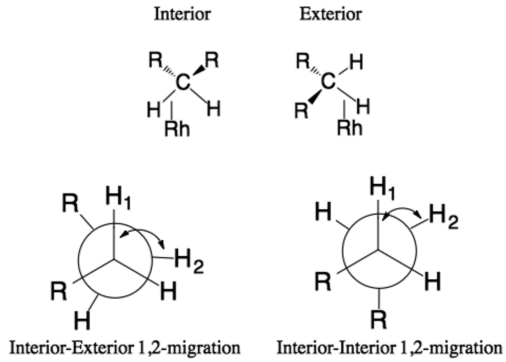

Cp*Rh(CO) Reactions. The differences between the Cp*Rh(CO) and CpRh(CO) reactions lie in a competition between the Cp* fragment's higher electron density and the increased steric repulsion associated with the additional methyl groups, and they are reflected in the transition state barriers as well as the stability of the σ-complexes. The σ-complexes for all four cycloalkanes with Cp*Rh(CO) have shorter C−H bonds as well as longer Rh−C and Rh−H distances than for its Cp counterpart, Figure 11, which reflects a weaker interaction between the C−H bond and the Rh. As a consequence, the energy barriers for the most rapid ring migrations between σ-complexes were found to be lower, while a few of the migrations experienced more crowding for Cp*Rh(CO). Again, the 1,1-migrations were the only barriers included in the cyclohexane reaction due to the redundancy of 1,2-migrations. For cycloheptane and cyclooctane, the four types of ring migrations were calculated; for most migrations the barriers were lower for the Cp*Rh(CO) migrations, and, as for the CpRh(CO) reactions, migration barriers were lower in free energy for cyclooctane than for cycloheptane. For both situations the lower migration barriers correlate with less stable σ-complexes. Compared to CpRh(CO), there was a consistent increase in the free energies of activation for all of the Cp*Rh(CO) σ-complexes, which was assigned to the increase in steric repulsions in the TSs associated with the bulkier Cp* ligand. With higher barriers for C−H activations and somewhat lower barriers for migrations, the overall rates for Cp*Rh(CO) reactions could be influenced more by ring migrations than those for the CpRh(CO) reactions.

dx.doi.org/10.1021/ja5014773 | J. Am. Chem. Soc. 2014, 136, 8614−8625

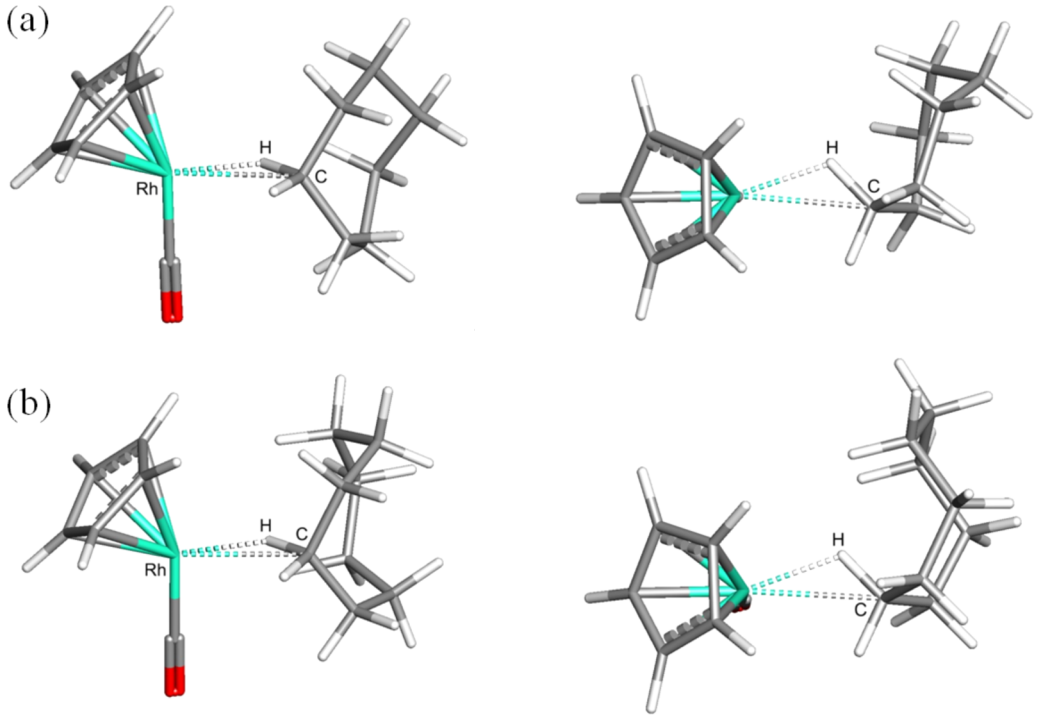

Figure 10. Side and top views of (a) the highest energy C(3)−H(5) cycloheptane and (b) the lowest energy C(1)−H(1) cyclooctane σ-complexes.

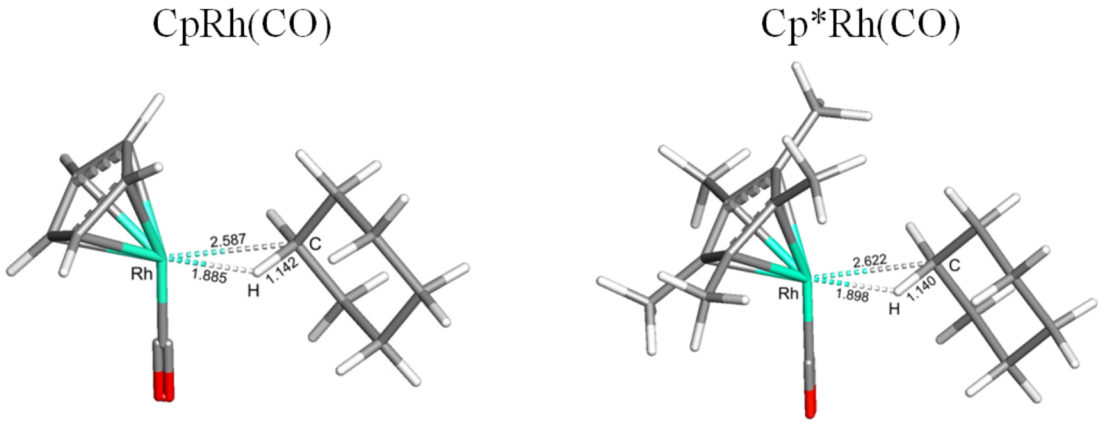

Figure 11. Comparison of the transition states for the cyclohexane C−H activation reaction with CpRh(CO) and Cp*Rh(CO).

Table 6. ns-TRIR Experimental and Simulated Lifetimes (ns) for the Static and Migration Mechanisms

	CpRh(CO)			Cp*Rh(CO)		
	static	migration	exptl	static	migration	exptl
cyclopentane	4.6	4.6	5.9(±0.2)	6.2	6.2	10.2(±0.8)
cyclohexane	14.9	14.7	8.6(±0.3)	34.3	30.8	25.8(±2.0)
cycloheptane	33.8	25.2	22.7(±0.7)	122.8	111.6	60.7(±2.4)
cyclooctane	44.3	37.4	31.7(±0.9)	170.2	125.9	74.3(±4.0)

SIMULATED MECHANISMS

Static Mechanism. Initially the σ-complexes were assumed to be statistically populated with all proceeding over the same attachment barrier. The static mechanism assumes that no ring migrations occur between σ-complexes, and each σ-complex proceeds over its own TS; i.e., activations are much faster than migrations, such that the latter can be neglected. The activation barriers were calculated for individual σ-complex/TS pairs where each σ-complex was its own zero relative energy. Predicted lifetimes with the static mechanism for all four cycloalkanes and both Rh fragments are compared with the experimental lifetimes in Table 6.

For cyclopentane there is only one C−H bond to activate, and therefore only one reaction mechanism can occur. The predicted lifetimes for the activation of cyclopentane with CpRh(CO) and Cp*Rh(CO) are 4.6 and 6.2 ns, respectively, which are similar to the experimental lifetimes of 5.9 and 10.2 ns. In the case of cyclohexane reacting with CpRh(CO), there were two pathways, axial and equatorial, which had an activation energy difference of 0.45 kcal mol^{-1}. Although this

dx.doi.org/10.1021/ja5014773 | J. Am. Chem. Soc. 2014, 136, 8614−8625

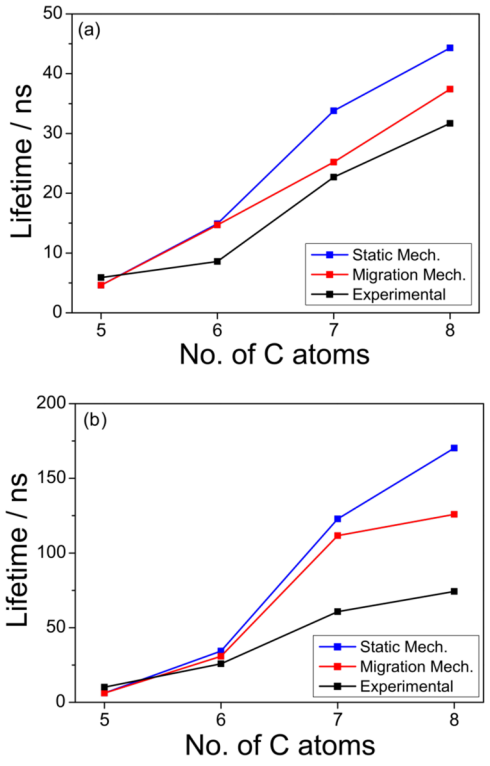

Figure 12. Calculated lifetimes for the four cycloalkane reactions with the static and migration mechanisms compared to the ns-TRIR measured lifetimes: (a) CpRh(CO) and (b) Cp*Rh(CO).

energy difference was small, the predicted lifetime for the axial pathway alone was 22.8 ns, while the lower energy, equatorial pathway predicted a lifetime of 10.9 ns. Including both pathways in the simulation, the predicted lifetime was 14.9 ns, which indicated that the majority of the product was initially formed by the equatorial species with a small contribution from the axial later in the reaction. The 14.9 ns lifetime for the CpRh(CO) reaction was slower than the experimental lifetime of 8.6 ns, Figure 12, and the difference between the cyclopentane and cyclohexane lifetimes was therefore overestimated. An axial/equatorial free energy difference of 0.70 kcal mol^{-1} for the Cp*Rh(CO) reaction was determined, so the small contribution from the axial pathway has a larger effect on the lifetime, which was predicted to be 34.3 ns. For cycloheptane, the simulated lifetimes of 33.8 and 122.8 ns for the CpRh(CO) and Cp*Rh(CO) reactions are in agreement with their respective experimental trends. The simulated cyclooctane lifetimes were 44.3 and 170.2 ns for CpRh(CO) and Cp*Rh(CO), respectively, which are longer than the experimental lifetimes of 31.7 and 74.3 ns, especially for Cp*Rh(CO). This overestimation also produces a slope between cycloheptane and cyclooctane that is too large for the Cp*Rh(CO) reaction. However, most of the migration barriers for cyclooctane are lower in energy than the activation barriers, so the migration mechanism will help correct this lifetime overestimation.

Migration Mechanism. The migration mechanism incorporates the calculated ring migrations between σ-complexes for each reaction into the overall activation mechanism, while the activation barriers remained the same as those for the static mechanism. Predicted lifetimes using the migration mechanism for the eight reactions are compared to the experimental lifetimes in Table 6.

Cyclopentane was not recalculated with this mechanism because ring migrations are truly redundant (since they lead to the activation of an equivalent C−H bond). For the cyclohexane and cycloheptane reactions, the predicted lifetimes show small decreases from those obtained with the static mechanism. The small decrease in the predicted lifetime for cyclohexane was solely due to the inclusion of the 1,1-migrations because they are the only transfers that are not redundant. With respect to the cycloheptane reactions, there was a larger contribution from other types of migrations, but the difference in the simulated lifetimes was not significant enough to conclude the importance of migrations in these reactions. Although the effect of migrations is similar for the cyclooctane reaction with CpRh(CO), the addition of migrations to the cyclooctane reaction with Cp*Rh(CO) correctly decreases the simulated lifetimes by 44.3 ns. This larger lifetime correction, which brings the predicted lifetime into closer alignment with the measured one, supports the conclusion that ring migrations contribute to the overall activation mechanism, particularly for cyclooctane with Cp*Rh(CO). Here, the steric crowding destabilizes the σ-complexes, which results in lower energy migration barriers and higher energy activation barriers, allowing the ring migrations to speed-up the reaction. Since the scaling factors were developed by using cyclohexane alone, one finds that the most sterically challenged reactions, Cp*Rh(CO) with larger cycloalkanes, have a larger error.

CONCLUSION

Despite all cycloalkanes being solely comprised of secondary CH_2 groups, a complicated step-like trend was observed in the ns-TRIR lifetimes for C−H activation, indicating that the overall picture was nontrivial. Calculations showed that with an increase in cycloalkane ring size there was an increase in the number of unique C−H bonds that can be activated. The different C−H bonds form a range of σ-complex stabilities and activation barriers, and these ranges widen with ring size. It is this large number of inequivalent C−H bonds and the larger steric crowding for the cycloheptane ring that leads to its large increase in lifetime.

As the energy range increases, ring migrations become more important as a way to reach the lower energy pathway. Populating the σ-complexes with the lowest energy activation barrier reduces the overall lifetime, but for this to be kinetically important, the migration barriers must be lower than the activation barriers. For cyclopentane and cyclohexane, there is essentially no decrease in lifetime with the inclusion of ring migrations in the reaction mechanism because the barriers for migrating around the ring are higher than the C−H activation barriers and also result in redundant exchanges. For the cycloheptane and cyclooctane reactions, the addition of ring migrations shortens the lifetimes of their σ-complexes as it allows these complexes to rearrange and proceed over lower C−H activation barriers. This difference is particularly important for cyclooctane reacting with Cp*Rh(CO); here, the increased steric crowding leads to less stable σ-complexes and therefore higher energy activation barriers and lower energy migration barriers. The energy changes for these two key barriers are large enough to allow the rhodium to migrate more rapidly between σ-complexes before activation in the cyclooctane reaction. Because the need to include ring migrations to describe the overall mechanism appears to be related to the size of the cycloalkane, we propose that in rings

dx.doi.org/10.1021/ja5014773 | J. Am. Chem. Soc. 2014, 136, 8614−8625

larger than cyclooctane the lifetimes would also show that ring migrations influence the rate of C−H activation.

■ ASSOCIATED CONTENT

Supporting Information

Energy scaling procedures, scaled and unscaled free energy barriers for C−H activations and σ-complex migrations, and Cartesian coordinates for all 160 structures described in the text. This material is available free of charge via the Internet at http://pubs.acs.org.

■ AUTHOR INFORMATION

Corresponding Authors

mike.george@nottingham.ac.uk
mbhall@tamu.edu

Notes

The authors declare no competing financial interest.

■ ACKNOWLEDGMENTS

M.B.H. thanks the National Science Foundation (CHE 0910552 and 1300787) for their financial support and the Texas A&M Supercomputer Facility for a generous allocation of computer time, A.W. thanks the University of Nottingham for funding, and M.W.G. gratefully acknowledges receipt of a Royal Society Wolfson merit award.

■ REFERENCES

(1) Janowicz, A. H.; Bergman, R. G. *J. Am. Chem. Soc.* **1982**, *104*, 352.
(2) Hoyano, J. K.; Graham, W. A. G. *J. Am. Chem. Soc.* **1982**, *104*, 3723.
(3) Crabtree, R. H. *J. Chem. Soc., Dalton Trans.* **2001**, 2437−2450.
(4) Bergman, R. G. *Nature* **2007**, *446*, 391.
(5) Labinger, J. A.; Bercaw, J. E. *Nature* **2002**, *417*, 507.
(6) Shilov, A. E.; Shul'pin, G. B. *Chem. Rev.* **1997**, *97*, 2879.
(7) (a) Castro-Rodriguez, I.; Nakai, H.; Gantzel, P.; Zakharov, L. N.; Rheingold, A. L.; Meyer, K. *J. Am. Chem. Soc.* **2003**, *125*, 15734. (b) Pike, S. D.; Thompson, A. L.; Algarra, A. G.; Apperley, D. C.; Macgregor, S. A.; Weller, A. S. *Science* **2012**, *337*, 1648.
(8) (a) Geftakis, S.; Ball, G. E. *J. Am. Chem. Soc.* **1998**, *120*, 9953. (b) Ball, G. E.; Brookes, C. M.; Cowan, A. J.; Darwish, T. A.; George, M. W.; Kawanami, H. K.; Portius, P.; Rourke, J. P. *Proc. Natl. Acad. Sci. U.S.A.* **2007**, *104*, 6927. (c) Lawes, D. J.; Darwish, T. A.; Clark, T.; Harper, J. B.; Ball, G. E. *Angew. Chem., Int. Ed.* **2006**, *45*, 4486.
(9) Calladine, J. A.; Torres, O.; Anstey, M.; Ball, G. E.; Bergman, R. G.; Curley, J.; Duckett, S. B.; George, M. W.; Gilson, A. I.; Lawes, D. J.; Perutz, R. N.; Sun, X.-Z.; Vollhardt, K. P. C. *Chem. Sci.* **2010**, *1*, 622.
(10) Bernskoetter, W. H.; Schauer, C. K.; Goldberg, K. I.; Brookhart, M. *Science* **2009**, *326*, 553.
(11) Young, R. D.; Lawes, D. J.; Hill, A. F.; Ball, G. E. *J. Am. Chem. Soc.* **2012**, *134*, 8294.
(12) Duckett, S. B.; George, M. W.; Jina, O. S.; Matthews, S. L.; Perutz, R. N.; Sun, X. Z.; Vuong, K. Q. *Chem. Commun.* **2009**, 1401.
(13) Calladine, J. A.; Duckett, S. B.; George, M. W.; Matthews, S. L.; Perutz, R. N.; Torres, O.; Khuong, Q. V. *J. Am. Chem. Soc.* **2011**, *133*, 2303.
(14) Creaven, B. S.; George, M. W.; Ginzburg, A. G.; Hughes, C.; Kelly, J. M.; Long, C.; McGrath, I. M.; Pryce, M. T. *Organometallics* **1993**, *12*, 3127.
(15) Calladine, J. A.; Vuong, K. Q.; Sun, X. Z.; George, M. W. *Pure Appl. Chem.* **2009**, *81*, 1667.
(16) Hermann, H.; Grevels, F. W.; Henne, A.; Schaffner, K. *J. Phys. Chem.* **1982**, *86*, 5151.
(17) Church, S. P.; Grevels, F. W.; Hermann, H.; Schaffner, K. *Inorg. Chem.* **1985**, *24*, 418.
(18) Childs, G. I.; Grills, D. C.; Sun, X. Z.; George, M. W. *Pure Appl. Chem.* **2001**, *73*, 443.
(19) George, M. W.; Turner, J. J. *Coord. Chem. Rev.* **1998**, *177*, 201.
(20) Schoonover, J. R.; Strouse, G. F. *Chem. Rev.* **1998**, *98*, 1335.
(21) Schultz, R. H.; Bengali, A. A.; Tauber, M. J.; Weiller, B. H.; Wasserman, E. P.; Kyle, K. R.; Moore, C. B.; Bergman, R. G. *J. Am. Chem. Soc.* **1994**, *116*, 7369.
(22) McNamara, B. K.; Yeston, J. S.; Bergman, R. G.; Moore, C. B. *J. Am. Chem. Soc.* **1999**, *121*, 6437.
(23) George, M. W.; Hall, M. B.; Jina, O. S.; Portius, P.; Sun, X.-Z.; Towrie, M.; Wu, H.; Yang, X.; Zaric, S. D. *Proc. Natl. Acad. Sci. U.S.A.* **2010**, *107*, 20178.
(24) George, M. W.; Hall, M. B.; Portius, P.; Renz, A. L.; Sun, X.-Z.; Towrie, M.; Yang, X. *Dalton Trans.* **2011**, *40*, 1751.
(25) Asbury, J. B.; Ghosh, H. N.; Yeston, J. S.; Bergman, R. G.; Lian, T. Q. *Organometallics* **1998**, *17*, 3417.
(26) Saillard, J.-Y.; Hoffmann, R. *J. Am. Chem. Soc.* **1984**, *106*, 2006.
(27) (a) Ziegler, T.; Tschinke, V.; Ursenbach, C. *J. Am. Chem. Soc.* **1987**, *109*, 4825. (b) Ziegler, T.; Tschinke, V.; Becke, A. D. *J. Am. Chem. Soc.* **1987**, *109*, 1351. (c) Ziegler, T.; Tschinke, V.; Versluis, L.; Baerends, E. J.; Ravenek, W. *Polyhedron* **1988**, *7*, 1625. (d) Ziegler, T.; Wendan, C.; Baerends, E. J.; Ravenek, W. *Inorg. Chem.* **1988**, *27*, 3458.
(28) Ziegler, T.; Tschinke, V.; Fan, L.; Becke, A. D. *J. Am. Chem. Soc.* **1989**, *111*, 9177.
(29) Song, J.; Hall, M. B. *Organometallics* **1993**, *12*, 3118.
(30) Cundari, T. R. *J. Am. Chem. Soc.* **1994**, *116*, 340.
(31) Low, J. J.; Goddard, W. A. *J. Am. Chem. Soc.* **1986**, *108*, 6115.
(32) Koga, N.; Morokuma, K. *J. Am. Chem. Soc.* **1990**, *94*, 5454.
(33) Balcells, D.; Clot, E.; Eisenstein, O. *Chem. Rev.* **2010**, *110*, 749.
(34) Niu, S.; Hall, M. B. *Chem. Rev.* **2000**, *100*, 353.
(35) Clot, E.; Eisenstein, O.; Jones, W. D. *Proc. Natl. Acad. Sci. U.S.A.* **2007**, *104*, 6939.
(36) Fischer, E. O.; Bittler, K. *Z. Naturforsch. B* **1961**, *16*, 225.
(37) Alamiry, M. A. H.; Boyle, N. M.; Brookes, C. M.; George, M. W.; Long, C.; Portius, P.; Pryce, M. T.; Ronayne, K. L.; Sun, X.-Z.; Towrie, M.; Vuong, K. Q. *Organometallics* **2009**, *28*, 1461.
(38) Frisch, M. J.; Trucks, G. W.; Schlegel, H. B.; Scuseria, G. E.; Robb, M. A.; Cheeseman, J. R.; Scalmani, G.; Barone, V.; Mennucci, B.; Petersson, G. A.; Nakatsuji, H.; Caricato, M.; Li, X.; Hratchian, H. P.; Izmaylov, A. F.; Bloino, J.; Zheng, G.; Sonnenberg, J. L.; Hada, M.; Ehara, M.; Toyota, K.; Fukuda, R.; Hasegawa, J.; Ishida, M.; Nakajima, T.; Honda, Y.; Kitao, O.; Nakai, H.; Veven, T.; Montgomery, J. A., Jr.; Peralta, J. E.; Ogliaro, F.; Bearpark, M.; Heyd, J. J.; Brothers, E.; Kudin, K. N.; Staroverov, V. N.; Kobayashi, R.; Normand, J.; Raghavachari, K.; Rendell, A.; Burant, J. C.; Iyengar, S. S.; Tomasi, J.; Cossi, M.; Rega, N.; Millam, J. M.; Klene, M.; Knox, J. E.; Cross, J. B.; Bakken, V.; Adamo, C.; Jaramillo, J.; Gomperts, R.; Stratmann, R. E.; Yazyev, O.; Austin, A. J.; Cammi, R.; Pomelli, C.; Ochterski, J. W.; Martin, R. L.; Morokuma, K.; Zakrzewski, V. G.; Voth, G. A.; Salvador, P.; Dannenberg, J. J.; Dapprich, S.; Daniels, A. D.; Farkas, O.; Foresman, J. B.; Ortiz, J. V.; Cioslowski, J.; Fox, D. J. *Gaussian 09*, Revision A.02; Gaussian, Inc.: Wallingford, CT, 2009.
(39) Boese, A. D.; Martin, J. M. L. *J. Chem. Phys.* **2004**, *121*, 3405.
(40) Becke, A. D. *J. Chem. Phys.* **1993**, *98*, 5648.
(41) Lee, C.; Yang, W.; Parr, R. G. *Phys. Rev. B: Condens. Matter* **1988**, *37*, 785.
(42) Chai, J.-D.; Head-Gordon, M. *Phys. Chem. Chem. Phys.* **2008**, *10*, 6615.
(43) Tao, J. M.; Perdew, J. P.; Staroverov, V. N.; Scuseria, G. E. *Phys. Rev. Lett.* **2003**, *91*, 146401.
(44) Becke, A. D. *Phys. Rev. A* **1988**, *38*, 3098.
(45) Perdew, J. P. *Phys. Rev. B* **1986**, *34*, 7406.
(46) Perdew, J. P.; Burke, K.; Ernzerhof, M. *Phys. Rev. Lett.* **1996**, *77*, 3865.
(47) Perdew, J. P.; Burke, K.; Ernzerhof, M. *Phys. Rev. Lett.* **1997**, *78*, 1396.
(48) Grimme, S. *J. Comput. Chem.* **2006**, *27*, 1787.
(49) Zhao, Y.; Truhlar, D. G. *J. Chem. Phys.* **2006**, *125*, 1.
(50) (a) Krishnan, R.; Binkley, J. S.; Seeger, R.; Pople, J. A. *J. Chem. Phys.* **1980**, *72*, 650. (b) McLean, A. D.; Chandler, G. S. *J. Chem. Phys.* **1980**, *72*, 5639.

(51) Clark, T.; Chandrasekhar, J.; Spitznagel, G. W.; Schleyer, P. v. R. *J. Comput. Chem.* **1983**, *4*, 294.
(52) (a) Andrea, D.; Haeussermann, U.; Dolg, M.; Stoll, H.; Preuss, H. *Theor. Chim. Acta* **1990**, *77*, 123. (b) Martin, J. M. L.; Sundermann, A. *J. Chem. Phys.* **2001**, *114*, 3408.
(53) Cossi, M.; Rega, N.; Scalmani, G.; Barone, V. *J. Comput. Chem.* **2003**, *24*, 669.
(54) (a) Manson, J.; Webster, C. E.; Hall, M. B. *JIMP2*, Version 0.091, a free program for Visualizing and manipulating molecules; Texas A&M University: College Station, TX, 2006. (b) Hall, M. B.; Fenske, R. F. *Inorg. Chem.* **1972**, *11*, 768.
(55) Hinsberg, W.; Houle, F.; Allen, F.; Yoon, E. *Chemical Kinetics Simulator 1.0.1*; International Business Machines Corp.: Alamaden, CA, 1998.
(56) Krug, X.; Hunter, Y.; Grieger, Z. *J. Phys. Chem.* **1976**, *80*, 2335.
(57) Liu, X.; Guo, X. *Chem. Rev.* **2001**, *101*, 673.